Cell

Regulation of Circadian Behavioral Output via a MicroRNA-JAK/STAT Circuit

Wenyu Luo[1] and Amita Sehgal[1,2,*]
[1]Cell and Molecular Biology Program
[2]Department of Neuroscience, Howard Hughes Medical Institute
University of Pennsylvania School of Medicine, Philadelphia, PA 19104, USA
*Correspondence: amita@mail.med.upenn.edu
DOI 10.1016/j.cell.2011.12.024

SUMMARY

Although molecular components of the circadian clock are known, mechanisms that transmit signals from the clock and produce rhythmic behavior are poorly understood. We find that the microRNA *miR-279* regulates the JAK/STAT pathway to drive rest:activity rhythms in *Drosophila*. Overexpression of microRNA *miR-279* or *miR-279* deletion attenuates rest:activity rhythms. Oscillations of the clock protein PERIOD are normal in pacemaker neurons lacking *miR-279*, suggesting that *miR-279* acts downstream of the clock. We identify the JAK/STAT ligand, *Upd*, as a target of *miR-279* and show that knockdown of *Upd* rescues the behavioral phenotype of *miR-279* mutants. Manipulations of the JAK/STAT pathway also disrupt circadian rhythms. In addition, central clock neurons project in the vicinity of *Upd*-expressing neurons, providing a possible physical connection by which the central clock could regulate JAK/STAT signaling to control rest:activity rhythms.

INTRODUCTION

The endogenous system that generates circadian rhythms has historically been depicted in the form of a heuristic model in which an endogenous clock receives environmental signals through an input pathway and transmits signals through an output pathway (Eskin, 1979). Rest:activity rhythms are the ultimate output of such a system. The past two decades have seen major advances in our understanding of how an endogenous clock is assembled and how the clock perceives the primary synchronizing/entraining signal, light (Zheng and Sehgal, 2008). However, the pathway that carries time-of-day signals away from the clock to produce overt circadian rhythms is less well understood.

Cellular and metabolic output pathways have been characterized in a variety of organisms (Asher and Schibler, 2011; Harmer, 2009; Vitalini et al., 2006). However, the components that control the overt rhythm of animal rest:activity have been more challenging to identify. Compared to other animals, flies have a relatively simple nervous system, but the circadian system still involves many different cell types in a neural network (Nitabach and Taghert, 2008). The most successful method used to identify clock molecules in *Drosophila*—forward genetic screens—have had limited success in identifying output molecules. This may be because many clock components are primarily dedicated to timekeeping, and loss of them is not lethal, whereas most output components are likely to be involved in essential functions including signal transduction and synaptic transmission. To date, only a limited number of output molecules have been implicated in rest:activity rhythms, and most of these have not been placed in specific signaling pathways (Allada and Chung, 2010).

MicroRNAs (miRNAs) are a class of small, noncoding RNAs that negatively regulate target gene expression (Carthew and Sontheimer, 2009). It is becoming increasingly clear that most biological processes involve regulation by miRNAs. This should be particularly true for circadian rhythms, where maintenance of appropriate protein levels can be critical for timekeeping. For instance, in *Drosophila,* the loss of or overexpression of the rhythmically expressed clock genes *period* and *timeless* results in arrhythmia (Yang and Sehgal, 2001; Zheng and Sehgal, 2008). Although recent work has identified miRNAs that regulate circadian rhythms in both mammals and flies (Cheng et al., 2007; Kadener et al., 2009; Kojima et al., 2010; Shi et al., 2009; Yang et al., 2008), the few miRNAs that are linked to rest:activity rhythms are implicated in clock function or clock input but not clock output (Cheng et al., 2007; Kadener et al., 2009).

Here, we report the identification of a miRNA, *miR-279*, whose loss does not affect the central clock but attenuates rest:activity rhythms, indicating that it is part of the output pathway. We identify the circadian-relevant target of this miRNA as *Unpaired* (*Upd*), the ligand for the JAK/STAT pathway, and find that manipulations of JAK/STAT signaling disrupt rest:activity rhythms. Moreover, we show that the central clock neurons project in the vicinity of cells that express *Upd*. This is consistent with central clock control of *miR-279*-regulated JAK/STAT signaling output, which, in turn, drives rest:activity rhythms. Together these findings demonstrate a role for JAK/STAT signaling in circadian rhythms and identify cellular and molecular components of a circuit that regulates circadian behavioral output.

RESULTS

Identification of *miR-279* as a Circadian Rhythm-Affecting MicroRNA

To identify genes affecting locomotor activity rhythms, we previously performed a forward genetic screen of 3,662 EP (enhancer

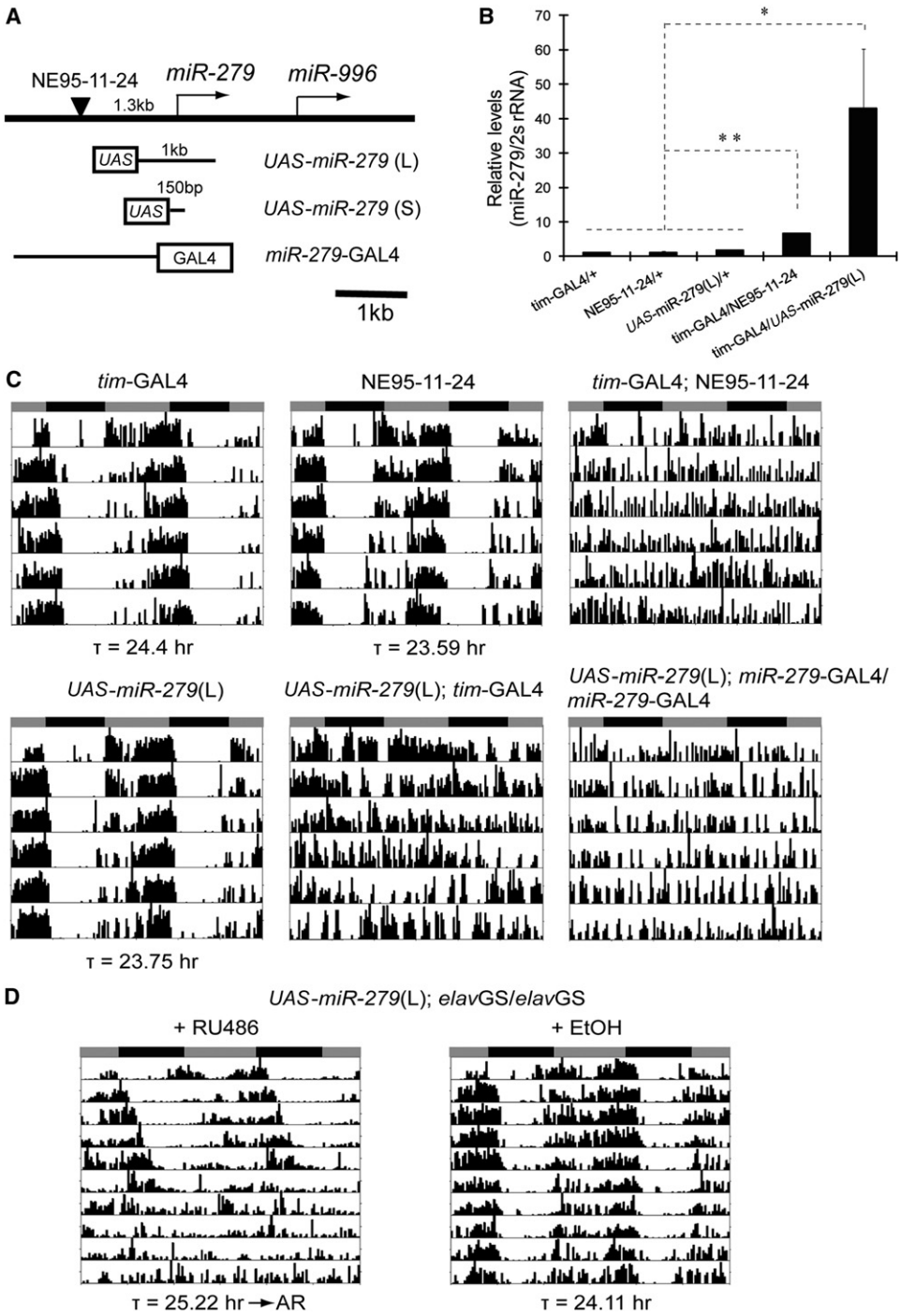

Figure 1. Overexpression of *miR-279* Disrupts Locomotor Activity Rhythms

(A) Map of the *miR-279* locus and transgenic constructs. An EP element (NE95-11-24, black triangle) is mapped 1.3 kb upstream of *miR-279*. Two *UAS-miR-279* transgenic lines were generated with a 1 kb (L) or a 150 bp (S) genomic region of *miR-279* fused to *UAS*. A *miR-279*-GAL4 reporter (Cayirlioglu et al., 2008) comprises the entire promoter of *miR-279* fused to GAL4.

(B) Overexpression of *miR-279* by driving expression of NE95-11-24 or a *UAS-miR-279* (L) transgene. Bars depict qPCR analysis of total RNA prepared from adult heads. The ratio of mature *miR-279*/2s rRNA was plotted as mean ± standard deviation (SD) (**$p < 0.001$, *$p < 0.01$, by Student's t test). Levels were normalized relative to the levels seen in *tim*G4/+ control flies (set as 1).

(C) Overexpression of *miR-279* leads to behavioral arrhythmia in DD. The genotypes are indicated on top of the panels. The gray and black bars indicate subjective day and night, respectively. Average periods (τ) of rhythmic flies are shown at the bottom of the panels. Representative activity records are shown.

Table 1. Alterations in Levels of *miR-279* Disrupt Locomotor Rhythms in Flies

Genotype	R % (n)[a]	Period ± SEM (hr)	FFT ± SEM
tim-GAL4/+	100 (18/18)	24.4 ± 0.07	0.122 ± 0.009
NE95-11-24/+	100 (26/26)	23.59 ± 0.03	0.135 ± 0.011
tim-GAL4/+; NE95-11-24/+	0 (0/26)	—	—
UAS-miR-279(S)/Y	100 (51/51)	23.8 ± 0.03	0.111 ± 0.006
UAS-miR-279(L)/Y	100 (28/28)	23.75 ± 0.04	0.099 ± 0.007
UAS-miR-279(S)/Y; *tim*-GAL4/+	2.1 (1/48)	24.67	0.05
UAS-miR-279(L)/Y; *tim*-GAL4/+	30 (6/20)	25.28 ± 0.17	0.037 ± 0.007
miR-279-GAL4/*miR-279*-GAL4	90 (18/20)	23.65 ± 0.06	0.035 ± 0.005
miR-279-GAL4/*miR-279*-GAL4; NE95-11-24/+	0 (0/12)	—	—
UAS-miR-279(S)/Y; *miR-279*-GAL4/*miR-279*-GAL4	11.1 (2/18)	24.08 ± 0.75	0.015 ± 0.002
UAS-miR-279(L)/Y; *miR-279*-GAL4/*miR-279*-GAL4	0 (0/7)	—	—
*elav*GS/*elav*GS (+EtOH)	100 (8/8)	23.96 ± 0.12	0.095 ± 0.018
*elav*GS/*elav*GS (+RU486)	100 (7/7)	24.63 ± 0.13	0.069 ± 0.015
UAS-miR-279(S)/Y; *elav*GS/*elav*GS (+EtOH)	87.5 (7/8)	24.13 ± 0.09	0.048 ± 0.009
UAS-miR-279(S)/Y; *elav*GS/*elav*GS (+RU486)	0 (0/8)[b]	25.42 ± 0.07[b]	0.038 ± 0.009[b]
UAS-miR-279(L)/Y; *elav*GS/*elav*GS (+EtOH)	100 (8/8)	24.11 ± 0.09	0.081 ± 0.014
UAS-miR-279(L)/Y; *elav*GS/*elav*GS (+RU486)	0 (0/8)[b]	25.22 ± 0.12[b]	0.056 ± 0.01[b]
w^{1118} (sibling)	100 (21/21)	23.72 ± 0.04	0.095 ± 0.011
$miR\text{-}279^{ex117\text{-}1/ex117\text{-}1}$	33.3 (7/21) [c]	23.79 ± 0.28[c]	0.031 ± 0.008[c]
genomic *miR-279*/genomic *miR-279*; $miR\text{-}279^{ex117\text{-}1/ex117\text{-}1}$	95.5 (21/22)	23.82 ± 0.08	0.103 ± 0.008

[a] Flies showing a fast fourier transform (FFT) value > 0.01 are counted as rhythmic (R). The average periods and FFTs shown represent the average ± standard error of the mean (SEM) for all rhythmic flies.
[b] The flies became arrhythmic 4–5 days after transferring to DD. Periods and FFTs during the first 5 days in DD are shown.
[c] Only those flies surviving more than 5 days in DD were included.

and promoter) lines in which expression of each randomly inserted EP element was driven by a *timeless*-GAL4 driver (*tim*-GAL4) (Zheng et al., 2007). One strain (NE95-11-24) that displayed a disrupted locomotor activity rhythm in this screen contains an EP-element insertion 1.3 kb upstream of a microRNA gene, *miR-279* (Figures 1A and 1C; Table 1).

The *miR-279* gene mediates development of *Drosophila* CO_2 sensory neurons in the antenna through downregulation of the transcription factor Nerfin-1 (Cayirlioglu et al., 2008); however, it was recently identified as one of several microRNAs that are expressed highly in *tim* neurons (Kadener et al., 2009). To examine whether *miR-279* levels were increased by expression of NE95-11-24, we conducted quantitative real-time PCR (qPCR) analysis of total RNA from heads of flies expressing NE95-11-24 under the control of *tim*-GAL4. As shown in Figure 1B, *miR-279* RNA was more abundant in these flies than in wild-type controls. Because a second microRNA gene, *miR-996*, located 1.6 kb downstream of *miR-279* (Figure 1A), could also be induced by the *tim*-GAL4 driver, we asked whether overexpression of *miR-279* alone was responsible for the circadian rhythm phenotype. Thus, we generated transgenic *miR-279*-expressing lines in which either a 1 kb (L) or a 150 bp (S) genomic sequence that fully covers the *miR-279*-coding region was fused to an upstream activating sequence (*UAS*) (*UAS-miR-279*, Figure 1A). In combination with *tim*-GAL4, *UAS-miR-279* also increased expression of *miR-279* and led to arrhythmic locomotor activity in most flies (Figures 1B and 1C; Table 1). The few flies that maintained weak rhythms showed a slightly longer period than controls (Table 1).

To exclude the possibility that the behavioral phenotype was caused by ectopic induction of *miR-279* in neurons where it is normally not expressed, we utilized a GAL4 driver under the control of the *miR-279* promoter (Cayirlioglu et al., 2008) (Figure 1A and Figure S1A available online). Because *miR-279*-GAL4 is much weaker than *tim*-GAL4, we used two copies of this driver to induce *miR-279* overexpression. As shown in Figure 1C and Table 1, overexpression of *miR-279* by *miR-279*-GAL4 phenocopies the effect of *tim*-GAL4, suggesting that *miR-279* regulates circadian rhythms in regions of its normal expression. To distinguish between developmental and adult effects of *miR-279*, we used two different approaches to restrict the expression of *miR-279* to adult neurons. We first drove its expression with a drug (RU486) inducible panneuronal driver, *elav*GeneSwitch (*elav*GS) (McGuire et al., 2004), which

(D) Panneuronal induction of *miR-279* in adulthood leads to a long period, which eventually degenerates into arrhythmia. Flies were reared and then aged for 3 days following eclosion on regular food. They were fed either 500 μM RU486 or ethanol (EtOH, vehicle control) from the time of entrainment. Average periods of the first 5 days in DD (τ) are shown beneath the panels.
See also Figure S1.

lengthened the period by ~0.6 hr during the first 5 days in constant darkness (DD) and then eventually caused arrhythmia (Figure 1D; Table 1). To determine the effects of adult expression in specific neurons, we used a temperature-sensitive *tubulin*-GAL80^{ts} coupled with a *tim*-GAL4 driver (*tim-UAS*-GAL4, TUG) (Blau and Young, 1999) or with *miR-279*-GAL4. The TUG driver is weaker than the *tim*-GAL4 used above (data not shown) and thus can be effectively repressed by *tubulin*-GAL80^{ts} at 18°C. Adult-specific overexpression of *miR-279* in *tim* or *miR-279* cells, by shifting flies carrying these constructs to 29°C, also resulted in long periods and arrhythmicity (Figure S1B). Although the phenotype was somewhat weaker than that produced by constitutive overexpression of *miR-279*, suggesting some developmental contribution, these data nevertheless indicate that adult overexpression of *miR-279* in relevant cells attenuates circadian behavioral rhythms.

A Loss-of-Function Mutation in *miR-279* Disrupts Behavioral Rhythms

Deletions of the *miR-279* gene were generated by imprecise excisions of two different P element insertions, both of which are downstream of *miR-279* (Cayirlioglu et al., 2008). Loss of *miR-279* expression was reported to cause lethality at the late pupal stage in its original background (Cayirlioglu et al., 2008). We observed the same lethality in the *ex36-2* (1.9 kb deletion) flies after outcrossing to an isogenic w^{1118} background; however, a small percentage of outcrossed *ex117-1* flies (1.2 kb deletion, Figure 2A) survive up to 2 weeks as adults, thus allowing us to perform behavioral analysis.

qPCR analysis showed that brains of homozygous *ex117-1* flies do not express any detectable levels of *miR-279* (Figure 2B). Behavioral analysis of these flies revealed that ~67% of the flies have very weak to no rhythms in DD (Figure 2C; Table 1). A previously identified phenotype of these flies—ectopic CO_2 neuron formation—was rescued by a 3 kb genomic *miR-279* transgene (Cayirlioglu et al., 2008). We found that the same genomic construct also rescued the locomotor activity rhythm phenotype of *ex117-1* (Figures 2A and 2C; Table 1), indicating that the *miR-279* gene is responsible for the behavioral phenotype of *ex117-1* and is necessary for circadian rhythms.

The *miR-279* Mutation Does Not Affect the Central Clock

A central pacemaker in the small ventral lateral neurons (sLNvs) of the *Drosophila* brain drives free-running locomotor activity rhythms in DD (Nitabach and Taghert, 2008). To determine whether *miR-279* affects the central pacemaker itself or acts on downstream output pathways that ultimately drive locomotor rhythms, we assayed oscillations of the central clock protein, PERIOD (PER), in sLNvs of *ex117-1* adult flies. Entrained *ex117-1* and sibling control flies were placed in DD and subjected to immunocytochemistry of brain whole mounts on the 1st and 3rd days in DD. As shown in Figures 2D and S2A, mutant flies and wild-type controls exhibit similar daily PER cycling in sLNvs. No obvious differences in protein levels or protein localization were found at any time point assayed. Furthermore, PER oscillations in other major clock neuron groups, including dorsal lateral neurons (LNds) and group 1 dorsal neurons (DN1s), were also robust and synchronized between the two hemispheres in mutant fly brains (data not shown). In addition, loss of *miR-279* does not alter the viability or morphology of any known clock neuron groups nor the expression of pigment-dispersing factor (PDF), a neuropeptide expressed in LNvs (Figures 2D and S2B). The absence of a GFP signal in sLNvs of *miR-279*-GAL4:*UAS*-nuclear GFP (nGFP) flies (Figure S1A) further supports the idea that *miR-279* does not function in the central pacemaker, but rather in output pathways.

To test whether the expression of *miR-279* itself is regulated by the circadian clock, we examined levels of mature *miR-279* over the course of a light:dark cycle (LD) and in DD. Under neither condition was significant cycling of *miR-279* detected (Figure S2C and data not shown). Also, levels of *miR-279* were not altered in clock gene mutants tim^{01} and Clk^{Jrk} (Figure S2D). The results suggest that levels of *miR-279* are not controlled by the circadian clock.

miR-279 Targets *Unpaired* to Regulate Circadian Behavioral Rhythms

With few exceptions, animal miRNAs recognize miRNA-binding sites in the 3′ untranslated regions (UTRs) of target mRNAs and cause mRNA degradation or translational repression (Carthew and Sontheimer, 2009). A previously identified target of *miR-279*, relevant for its effects on the development of CO_2 neurons, is the mRNA encoded by the Nerfin-1 gene (Cayirlioglu et al., 2008). We tested flies expressing a Nerfin-1 RNAi construct for circadian behavior and found that their behavioral rhythm was normal (data not shown), suggesting that Nerfin-1 does not mediate effects of *miR-279* on circadian rhythms. We therefore sought to identify other possible targets of *miR-279*. Using three computational algorithms (i.e., PicTar, TargetScanFly5.1, and MiRanda) (Krek et al., 2005; Ruby et al., 2007), we discovered that ~35 mRNAs contain putative binding sites for *miR-279* in their 3′ UTRs (Figure S3A; Table S1). We obtained fly stocks carrying RNAi knockdown constructs for each of these mRNAs from the NIG-FLY stock center (~75 lines), introduced a *tim*-GAL4 or a *miR-279*-GAL4 transgene into each stock, and screened the resulting progeny for locomotor rhythms. Rhythms were impaired when expression of the *Upd* gene was knocked down (Figures 3A and S3B).

Upd (also called *Outstretched*) mRNA was predicted as a potential target of *miR-279* by all three computational algorithms we employed (Table S1). In fact, the *Upd* 3′ UTR contains multiple putative *miR-279*-binding sites, one of which is highly conserved across different *Drosophila* species (Figures 3B and 3C). To determine whether *miR-279* directly binds to the *Upd* 3′ UTR and inhibits its expression, we performed a luciferase reporter assay in *Drosophila* S2 cells. A chimeric mRNA was made by fusing the firefly luciferase open reading frame to the full-length *Upd* 3′ UTR that contains all potential *miR-279*-binding sites (Figure 3C). Compared to the control, luciferase activity of the chimeric mRNA was significantly suppressed when *miR-279* was cotransfected into the cells (Figure 3C). However, a mutant form of *miR-279,* in which sites complementary to those in the *Upd* 3′ UTR were altered (Figure 3B), failed to suppress luciferase activity (Figure 3C). We further examined whether *miR-279* affects *Upd* mRNA levels in vivo. As shown in Figure 3D, *Upd* mRNA was upregulated in adult brains of

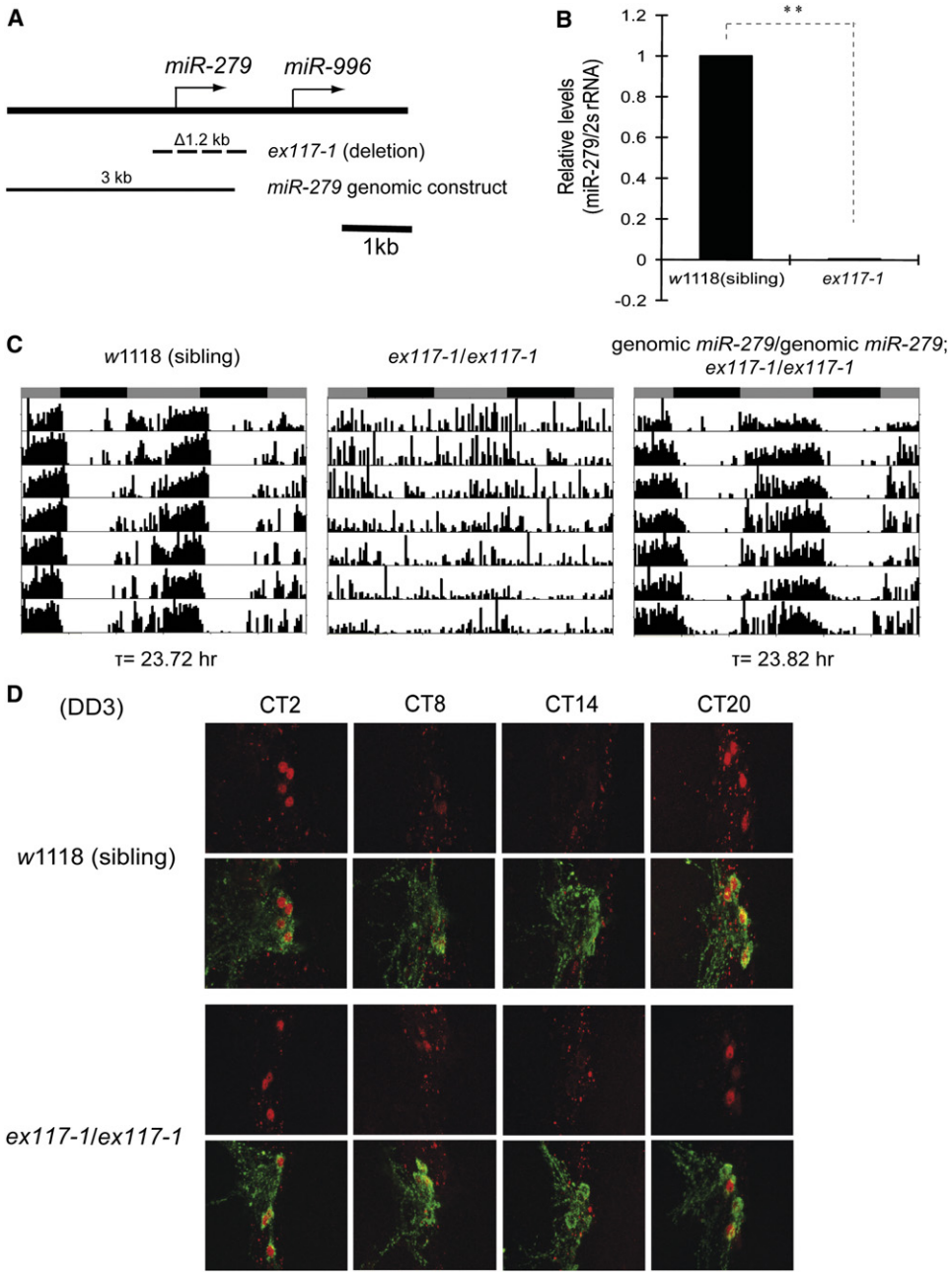

Figure 2. Deletion of *miR-279* Reduces Behavioral Rhythmicity without Changing PER Cycling in sLNvs

(A) The *miR-279* excision allele and genomic rescue construct (Cayirlioglu et al., 2008). The null allele *ex117-1* (dashed line, Δ1.2 kb) completely deletes the *miR-279* gene. The *miR-279* genomic construct (filled line, 3 kb) comprises the entire promoter and coding region of *miR-279*.

(B) The *ex117-1* allele completely abolishes production of mature *miR-279*. qPCR analysis of total RNA prepared from adult brains is shown. The ratio of mature *miR-279*/2s rRNA was plotted as mean ± SD (**$p < 0.001$, by Student's t test). Levels were normalized relative to those seen in w^{1118} control (set as 1).

(C) Deletion of *miR-279* disrupts activity rhythms, which can be rescued by introducing a *miR-279* genomic transgene. After being outcrossed seven times into a w^{1118} background, flies homozygous for *ex117-1* live up to 2 weeks as adults. w^{1118} flies derived from siblings during the last outcross were used as wild-type control (indicated as "sibling").

(D) The null allele of *miR-279* shows normal PER oscillations and PDF expression in central clock cells. Brains were dissected and stained with PER (red) and PDF (green) antibodies on the 3rd day of DD at the indicated circadian times (CT).

See also Figure S2.

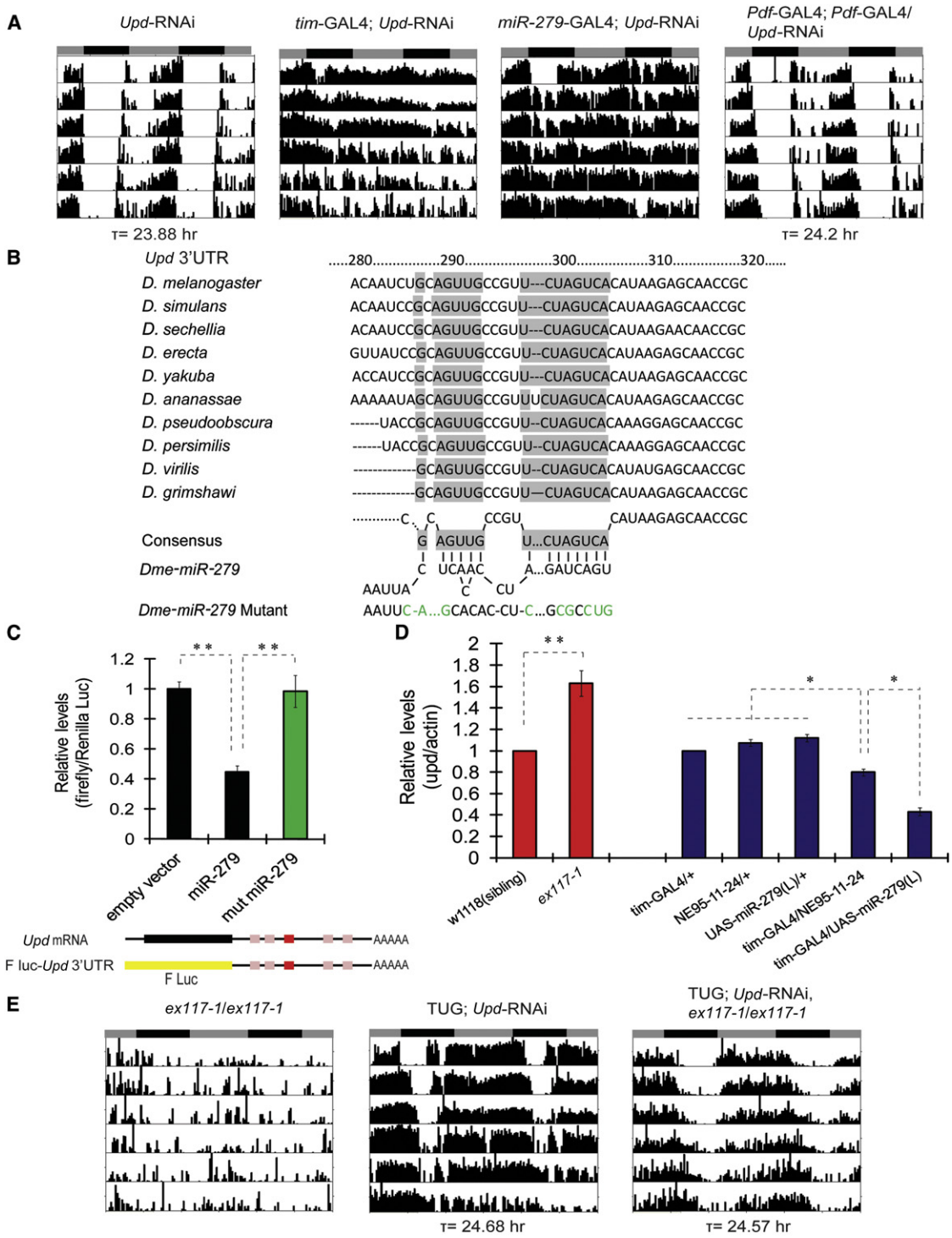

Figure 3. *Upd* Is a Direct Target of *miR-279*

(A) RNAi knockdown of the JAK/STAT ligand *Upd* abolishes behavioral rhythms. Expression of *Upd*-RNAi in either *miR-279* or *tim*-expressing neurons, but not in *Pdf* neurons, causes arrhythmia.

(B) A highly conserved 8 nucleotide *miR-279* target site in the 3′ UTR of *Upd* mRNA. A predicted *miR-279*-binding site (shaded boxes) is conserved within the 3′ UTR sequences of *Upd* mRNAs from different *Drosophila* species (TargetScanFly 5.1). Base-pairing between the consensus target site and the mature *miR-279* is shown. A *miR-279* mutant containing mismatched nucleotides (green) is shown at the bottom of the panel.

(C) *miR-279* inhibits expression of an *Upd* 3′ UTR-luciferase reporter in cultured *Drosophila* S2 cells. The entire 750 bp sequence of the *Upd* 3′ UTR, containing one conserved 8-mer (red box, by TargetScanFly 5.1) and four other putative *miR-279* target sites (pink boxes, by RNAhybrid), was fused to a firefly luciferase

Table 2. *miR-279* Acts through the JAK/STAT Pathway to Regulate Locomotor Activity Rhythms

Genotype	R % (n)	Period ± SEM (hr)	FFT ± SEM
*UAS-Upd*RNAi/+	100 (42/42)	23.88 ± 0.03	0.102 ± 0.005
tim-GAL4/+; *UAS-Upd*RNAi/+	21.4 (9/42)	24.83 ± 0.16	0.038 ± 0.005
miR-279-GAL4/+	100 (17/17)	23.53 ± 0.07	0.096 ± 0.008
miR-279-GAL4/+; *UAS-Upd*RNAi/+	42.9 (15/35)	24.04 ± 0.1	0.07 ± 0.008
Pdf-GAL4/+; *Pdf*-GAL4/+	100 (10/10)	24 ± 0.08	0.114 ± 0.012
Pdf-GAL4/+; *Pdf*-GAL4/*UAS-Upd*RNAi	100 (17/17)	24.2 ± 0.05	0.07 ± 0.008
TUG/+	100 (18/18)	24.06 ± 0.08	0.124 ± 0.012
TUG/+; *UAS-Upd*RNAi/+	86.7 (13/15)	24.68 ± 0.08	0.057 ± 0.007
TUG/TUG; *UAS-Upd*RNAi/+	42.1 (8/19)	26.12 ± 0.25	0.044 ± 0.006
miR-279$^{ex117\text{-}1/ex117\text{-}1}$	33.3 (7/21)[a]	23.79 ± 0.28[a]	0.031 ± 0.008[a]
TUG/+; *UAS-Upd*RNAi, *miR-279*$^{ex117\text{-}1/ex117\text{-}1}$	91.7 (11/12)	24.57 ± 0.17	0.051 ± 0.012
UAS-Upd/+	100 (18/18)	23.57 ± 0.05	0.145 ± 0.009
tim-GAL4/*UAS-Upd*	0 (0/24)	—	—
UAS-Upd/+; *elav*GS/*elav*GS (+EtOH)	87.5 (14/16)	23.63 ± 0.09	0.056 ± 0.009
UAS-Upd/+; *elav*GS/*elav*GS (+RU486)	33.3 (5/15)	23.45 ± 0.11	0.03 ± 0.011
Dome-GAL4/+	75 (12/16)	23.8 ± 0.12	0.031 ± 0.008
UAS-dome$^{\Delta CYT}$/+	100 (17/17)	23.28 ± 0.07	0.142 ± 0.015
Dome-GAL4/+; *UAS-dome*$^{\Delta CYT}$/+	15.4 (2/13)	24.09 ± 0.09	0.03 ± 0.009
tim-GAL4/*UAS-dome*$^{\Delta CYT}$	100 (16/16)	23.83 ± 0.05	0.192 ± 0.016
w^{1118} (sibling)	97.1 (34/35)	23.57 ± 0.05	0.088 ± 0.007
w^{1118}, *hop*^{25}/Y	32 (8/25)	23.62 ± 0.18	0.038 ± 0.005
UAS-hop^{Tuml}/+; *elav*GS/+ (+EtOH)	100 (10/10)	23.6 ± 0.09	0.085 ± 0.012
UAS-hop^{Tuml}/+; *elav*GS/+ (+RU486)	16.7 (2/12)	23 ± 0.25	0.018 ± 0.002
Upd-GAL4/Y	100 (19/19)	23.7 ± 0.03	0.095 ± 0.006
UAS-NachBac/+	100 (15/15)	23.6 ± 0.06	0.08 ± 0.009
Upd-GAL4/Y; *UAS*-NachBac/+	26.7 (4/15)	23.77 ± 0.22	0.034 ± 0.009
UAS-dTrpA1/+ (21°C)	100 (16/16)	23.75 ± 0.07	0.05 ± 0.005
UAS-dTrpA1/+ (28°C)	100 (16/16)	23.69 ± 0.06	0.075 ± 0.009
Upd-GAL4/Y; *UAS*-dTrpA1/+ (21°C)	86.7 (13/15)	23.61 ± 0.07	0.034 ± 0.004
Upd-GAL4/Y; *UAS*-dTrpA1/+ (28°C)	35.7 (5/14)	23.28 ± 0.15	0.021 ± 0.003
UAS-shi^{TS}/+; *UAS-shi*^{TS}/+ (21°C)	93.8 (15/16)	24.01 ± 0.12	0.033 ± 0.004
UAS-shi^{TS}/+; *UAS-shi*^{TS}/+ (29°C)	100 (15/15)	23.31 ± 0.13	0.062 ± 0.008
Upd-GAL4/Y; *UAS-shi*^{TS}/+; *UAS-shi*^{TS}/+ (21°C)	93.3 (14/15)	23.96 ± 0.09	0.047 ± 0.007
Upd-GAL4/Y; *UAS-shi*^{TS}/+; *UAS-shi*^{TS}/+ (29°C)	100 (15/15)	24.63 ± 0.09	0.066 ± 0.01

[a] The *miR-279* mutant data shown here for comparison are the same as those in Table 1.

miR-279 null mutants. On the other hand, *miR-279* overexpression by a *tim*-GAL4 driver reduced mRNA levels of *Upd*, with a higher dose of *miR-279* producing a stronger effect (Figures 1B and 3D). We conclude that *Upd* is a direct target of *miR-279* in vitro and in vivo.

To test whether high levels of *Upd* were responsible for the activity rhythm phenotype of *miR-279* mutants, we reduced expression of *Upd* with the *Upd*-RNAi construct (Figure S3B) in an *ex117-1* background. As shown in Figure 3E and Table 2, knocking down *Upd* with a relatively weak *tim* promoter (TUG)

(F luc, yellow bar) reporter construct (shown beneath the panel). An empty vector or a wild-type or mutant *miR-279* (as shown in panel B) expression plasmid was cotransfected with the firefly luciferase reporter plasmid. *Renilla* luciferase was used as transfection control. The ratio of firefly/*Renilla* luciferase is plotted as mean ± SD of triplicate data points (**p < 0.001, by Student's t test). The control with the empty vector is set as 1.

(D) *miR-279* is a negative regulator of *Upd* mRNA in vivo. qPCR analysis of total RNA prepared from fly brains (red bars) or fly heads (blue bars) is shown. The level of *Upd* in *ex117-1* was normalized to that in w^{1118} control (set as 1, red bars). The levels of *Upd* in flies overexpressing *miR-279* were normalized to those in *tim*G4/+ control (set as 1, blue bars). The ratios of *Upd*/*Actin* mRNA are plotted as mean ± SD (**p < 0.001, *p < 0.01, by Student's t test).

(E) RNAi knockdown of *Upd* rescues the arrhythmia of *miR-279* nulls. TUG is a comparatively weak *tim*-GAL4 driver (see text). The *ex117-1* mutant and flies expressing *Upd*-RNAi with TUG alone served as controls.

See also Figure S3 and Table S1.

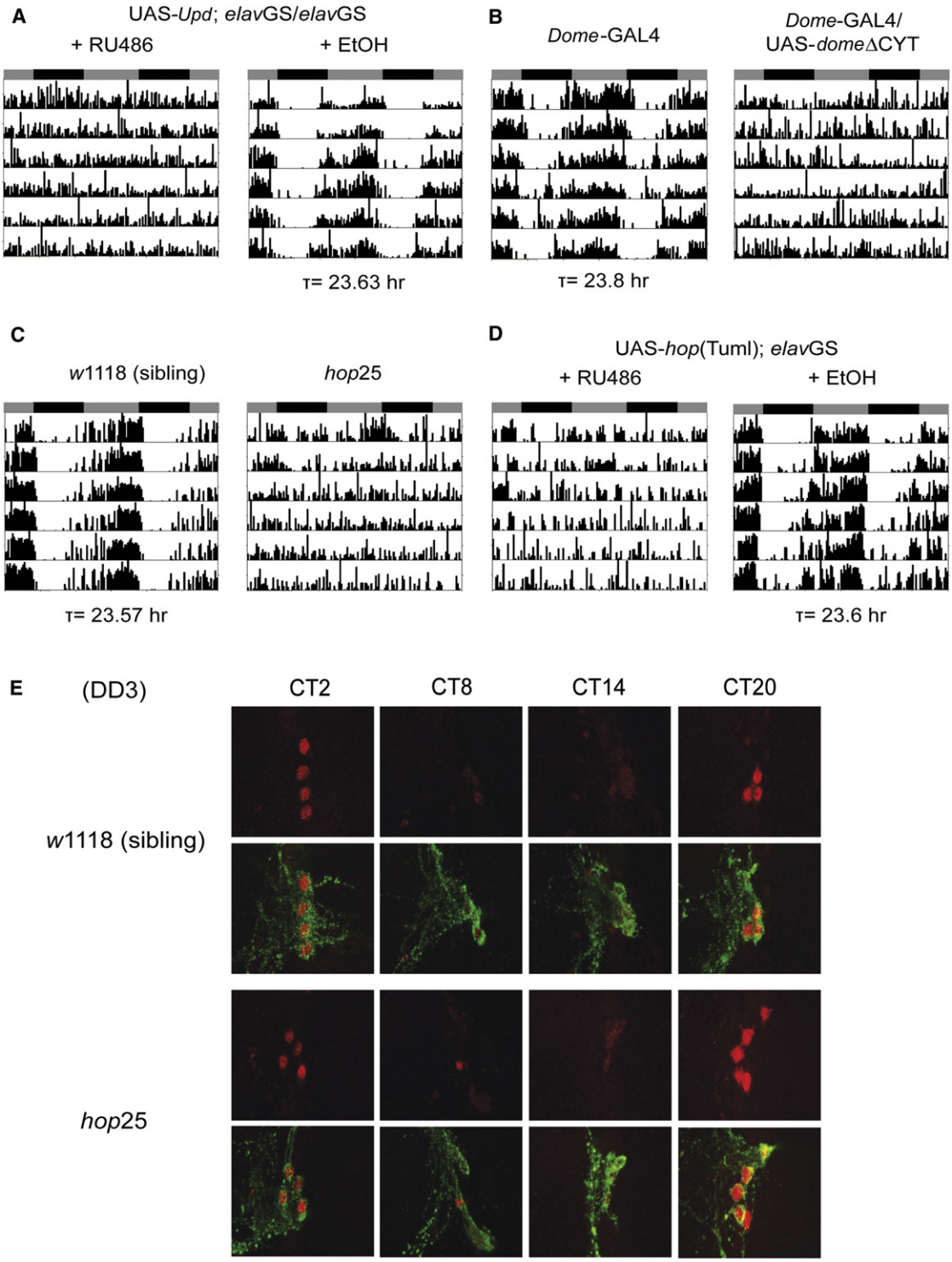

Figure 4. The JAK/STAT Signaling Pathway Is Required for Locomotor Activity Rhythms

(A) Panneuronal induction of *Upd* in adulthood leads to arrhythmia. Flies were reared on regular food. Five hundred micromoles of RU486 or ethanol (control) was administered in the food from the time of entrainment.

(B) Blocking JAK/STAT signaling with a dominant-negative form of the receptor *Domeless* ($dome^{\Delta CYT}$) leads to arrhythmia. The *Dome*-GAL4 driver (Ghiglione et al., 2002) causes lethality in males, and thus only females were tested.

(C) A hypomorphic mutation of JAK kinase *Hopscotch* (hop^{25}) causes loss of activity rhythms. The hop^{25} allele is a Q246K point mutation of the *Hop* gene (Luo et al., 1999).

prevented the abolition of activity rhythms in *ex117-1* flies. These data provide strong in vivo evidence that *miR-279* regulates circadian rhythms by modulating levels of *Upd*.

Manipulations of the JAK/STAT Pathway Affect Behavioral Rhythms

The *miR-279* target we identified, *Upd*, is one of the three cytokine ligands (i.e., *Upd*, *Upd2*, and *Upd3*) that activate the JAK/STAT signaling cascade in *Drosophila* (Arbouzova and Zeidler, 2006; Harrison et al., 1998). Compared to its mammalian counterpart, the canonical JAK/STAT pathway in *Drosophila* is relatively simple with only a few key components. Ligand binding activates a transmembrane receptor, DOMELESS (DOME), that recruits the Janus kinase protein HOPSCOTCH (HOP) to its intracellular domain. This allows HOP to phosphorylate itself, as well as the receptor DOME, and a cytoplasmic protein, signal transducers and activators of transcription (STAT92E). Upon phosphorylation by HOP, STAT92E dimerizes and translocates to the nucleus to regulate transcription (Arbouzova and Zeidler, 2006).

Given that *Upd* is part of the JAK/STAT pathway, we asked whether manipulating components of the JAK/STAT would alter locomotor activity rhythms in flies. As noted above, knockdown of *Upd* in clock neurons with the strong *tim*-GAL4 driver disrupted rhythms (Figure 3A; Table 2). A slow breakdown of rhythms was also observed with the *miR-279* driver (Figure 3A; Table 2). Because *tim*-GAL4 is expressed at higher levels but may show some ectopic expression (data not shown), we also tested two copies of the TUG driver, which likely better represents the circadian clock network. This manipulation also disrupted behavioral rhythms and produced overall high activity in wild-type flies (Table 2; notice higher activity in Figure 3E even with one copy of TUG). The *Upd*-RNAi transgene yielded no phenotype with the *Pdf*-GAL4 driver, even when two copies were used (Figure 3A; Table 2), indicating that *Upd* function is not restricted to *Pdf* neurons. Together, these data suggest that appropriate expression of *Upd* is required for normal rhythms; it needs to be downregulated but not completely abolished by *miR-279*, which is also consistent with the results of the in vitro luciferase reporter assay (Figure 3C). This conclusion is further supported by our findings that either constant high levels of *Upd* in *tim* neurons or induction of *Upd* in adults disrupts activity rhythms (Table 2; Figure 4A). Overexpression of *Upd* in *miR-279* neurons throughout development resulted in lethality (data not shown).

We next examined whether blocking signal transduction downstream of *Upd* affects behavioral rhythms. To investigate the role of DOME, we used a dominant-negative form of this receptor, DOME$^{\Delta CYT}$, which lacks the intracellular domain and the sites for HOP binding. The mutant receptor contains the extracellular and transmembrane portions of the protein and thus titrates the ligand and acts as a signaling antagonist (Brown et al., 2001). Expression of *UAS-dome*$^{\Delta CYT}$ under the control of a *Dome* promoter enhancer trap GAL4 (Ghiglione et al., 2002), but not *tim*-GAL4, dramatically reduced the percentage of rhythmic flies compared to controls (Table 2; Figure 4B), suggesting that normal activity rhythms require a ligand-responsive DOME receptor in non-*tim* neurons.

We further determined whether the Janus kinase HOP modulates circadian behaviors. Although complete amorphs of *Hop* are lethal, a small percentage of flies carrying a severe hypomorphic allele, *hop*^{25}, emerge as hemizygous males (Perrimon and Mahowald, 1986) and survive up to 2 weeks in an isogenic *w*^{1118} background. We found that ~68% of the *hop*^{25} males lost activity rhythms in constant darkness, whereas only 3% of wild-type sibling controls were arrhythmic (Figure 4C; Table 2). We also tested a dominant gain-of-function allele, *hopscotch*$^{\text{Tumorous-lethal}}$ (*hop*$^{\text{Tuml}}$), which produces a constitutively active form of HOP and causes hyperactivity of the JAK/STAT pathway (Harrison et al., 1995; Luo et al., 1995). Expression of *UAS-hop*$^{\text{Tuml}}$ by *elav*GS resulted in an acute disruption of locomotor activity rhythms in adults (Figure 4D; Table 2). To determine whether *Hop* also affects circadian output pathways downstream of the central clock, we assayed PDF expression and protein oscillations of PER in sLNvs of *hop*^{25} adult flies. Entrained *hop*^{25} and sibling control flies were subjected to immunocytochemistry of brain whole mounts on the 3rd day in DD. As shown in Figure 4E, mutant flies exhibit PDF expression and daily PER cycling in sLNvs that are similar to those of wild-type controls. All these data are consistent with a major role for JAK/STAT signaling in circadian outputs that drive rhythmic behaviors.

Modulation of *Upd*-Expressing Neurons Alters Behavioral Rhythms

To determine whether UPD-secreting neurons are important for circadian behaviors, we utilized an *Upd* enhancer trap GAL4 driver, *Upd* (E132)-GAL4 (Halder et al., 1995), and tested whether silencing or activating *Upd*-expressing neurons alters activity rhythms. Due to a critical role of *Upd* and JAK/STAT signaling in fly development (Harrison et al., 1998; Hou et al., 1996; Perrimon and Mahowald, 1986), inactivation of UPD-secreting cells by *Upd*-GAL4-controlled expression of an inward rectifying potassium channel, Kir2.1 (Baines et al., 2001), caused lethality (data not shown). To conditionally suppress *Upd* neurons at the adult stage, we expressed a temperature-sensitive synaptic blocker, *shibire*^{TS} (*shi*^{TS}), under the control of *Upd*-GAL4. The *shi*^{TS} allele is defective in synaptic vesicle recycling at restrictive temperatures (>29°C) and leads to a rapid and reversible inhibition of synaptic transmission (Koenig et al., 1983). Upon a shift to 29°C, the period of the activity rhythm was lengthened ~0.7 hr compared to that of control flies, and this phenotype reverted to normal after flies were transferred back to permissive temperature (21°C) (Figure S4A; Table 2).

(D) Overexpression of a constitutively active form of *Hop* (*hop*^{Tuml}) in the adult nervous system disrupts activity rhythms. The gain-of-function mutation *hop*^{Tuml} is a G341E single amino acid substitution in the *Hop* gene (Harrison et al., 1995; Luo et al., 1995).

(E) The *hop*^{25} mutants show normal PER cycling and PDF expression in central pacemaker neurons. Brains were dissected and stained with PER (red) and PDF (green) antibodies on the 3rd day of DD at the indicated circadian times (CT).

See also Figure S4.

The long period phenotype produced by blocking *Upd*-expressing neurons is consistent with the effects of *miR-279* overexpression, which lowers the level of *Upd,* in the small percentage of rhythmic flies (Figure 1D; Table 1). To confirm the importance of *Upd*-expressing neurons in regulating circadian rhythms, we then activated these neurons. Under the control of *Upd*-GAL4, the expression of a sodium channel, NaChBac, which depolarizes neurons and increases their excitability (Ren et al., 2001), abolished free-running rhythms in most flies (Table 2). In addition, acute excitation of *Upd* neurons in adult flies by activating a temperature-gated cation channel dTrpA1 at 28°C (Hamada et al., 2008) also disrupted activity rhythms (Figure S4B; Table 2). The effect of dTrpA1 was reversible, with normal rhythms restored at the permissive temperature of 21°C. We conclude that *Upd*-expressing cells are necessary for normal circadian locomotor rhythms.

JAK/STAT Signaling Cycles under the Control of the Circadian Clock

To test the hypothesis that JAK/STAT signaling is an output modulated by the circadian clock, we examined the expression profile of JAK/STAT components over the course of a circadian cycle in DD. Western blot assays of fly brain extracts were performed using antibodies specific for UPD, HOP, and STAT92E. Although no oscillations were detectable for the major bands corresponding to UPD and HOP proteins, a higher band, which may correspond to phosphorylated HOP, was expressed cyclically (Figure S5A). We also found that the fastest migrating form of STAT92E, which appears to be a doublet, was expressed cyclically on the 1st day in DD (Figures 5A–5C and S5B), with peak protein levels in the late day/early evening. STAT92E oscillations were dampened in clock gene mutants, more so in Clk^{Jrk} flies (Figure 5A) than in per^{01} flies (Figure S5B). The cycling of STAT92E persisted on the 2nd day of DD (Figure 5D), further supporting that it is under circadian control. STAT92E cycling was delayed in a null mutant of the PDF receptor (PDFR) $Pdfr^{han5304}$ (Hyun et al., 2005), suggesting that it is regulated by PDF signaling (Figure 5B). To determine whether JAK/STAT signaling and *miR-279* contribute to oscillations of STAT92E, we assayed STAT92E cycling in flies overexpressing hop^{Tuml} and also in the *miR-279* mutants. In both genotypes, the cycling of STAT92E was dampened, such that trough levels were increased (Figures 5C and 5D).

Because JAK/STAT signaling appears to be downstream of the central clock, we sought to determine whether *Upd*-expressing cells receive input from clock cells. We first labeled *Upd*-expressing neurons with nuclear-targeted GFP (nGFP) by crossing *UAS*-nGFP to *Upd*-GAL4 and found that *Upd* is expressed broadly in the adult fly brain. The expression pattern includes cells within two clusters of PER-positive neurons, DNs and some other neurons that we are calling lateral located neurons (LLNs) based upon their position (Figure 6A). Interestingly, the neurons in which *Upd* and PER expression overlap show shifted-phase PER cycling under LD conditions (i.e., protein levels are high in the early night and low in the early morning) (Figure 6A). We next expressed a cell membrane-targeted GFP (mCD8GFP) under the control of *Upd*-GAL4 and found that the PDF-containing dorsal projection from the small LNvs lies within clusters of *Upd*-expressing neurites (Figure 6B). As these projections are the ones typically associated with rest: activity output from small LNvs (Helfrich-Förster et al., 2000; Williams et al., 2001), these data are consistent with a role for *Upd*-expressing cells in this output. Using a Denmark reporter (Nicolaï et al., 2010), we also confirmed that the *Upd* neurites that contact the PDF projections are dendrites (Figure S6).

Finally, to visualize neurons receiving signals from UPD-secreting neurons, we expressed a mCD8GFP under the control of the *Dome*-GAL4 driver. As shown in Figure 6C, the expression pattern of *Dome* does not overlap with the major pacemaker neurons such as the small and large LNvs, LNds, and DN1s (Nitabach and Taghert, 2008), which is consistent with the lack of a phenotype when *UAS-dome*$^{\Delta CYT}$ is expressed by *tim*-GAL4 (Table 2). However, the GFP signal is enriched in other structures such as the Kenyon cell bodies and the α and β lobes of the mushroom bodies (MBs), the pars intercerebralis (PI), and a bilateral pair of dorsal giant interneurons (DGIs). Notably, the Kenyon cell bodies of the MBs are adjacent to the DNs and the PDF-containing dorsal projections of small LNvs (Figure 6C).

DISCUSSION

Although microRNAs play a critical role in most biological processes, few have been specifically implicated in circadian behavioral rhythms. In mammals, *miR-219* is involved in central clock function and *miR-132* in light input to the central clock (Cheng et al., 2007). In *Drosophila, bantam* miRNA affects free-running circadian rhythms by targeting the *Clock* gene (Kadener et al., 2009). We now isolate *miR-279* as an effecter of clock-controlled behavioral output, and we identify *Upd*, the ortholog of the JAK/STAT ligand, as the circadian-relevant target of this miRNA. We go on to show that manipulations of other components of the JAK/STAT pathway also disrupt behavioral rhythms, and we find that expression of STAT92E is rhythmic. Given the critical need for appropriate expression levels of *Upd*, we speculate that rhythms in STAT92E derive from circadian regulation at the level of *Upd*. Athough levels of UPD do not appear to cycle in whole brains (Figure S5A), cycling in specific cells cannot be excluded and secretion of UPD could be cyclic. Cyclic release of UPD would lead to rhythmic activation of DOME and thereby STAT92E (Figure 6D). Because STAT92E regulates its own expression through feedback (Arbouzova and Zeidler, 2006), rhythmic STAT92E activity is expected to result in cyclic expression, as reported here. PDF is also thought to be released cyclically (Park et al., 2000), and it regulates cycling of STAT92E (Figure 5B). This suggests control of the JAK/STAT pathway by central clock cells, which is supported by the proximity of PDF projections and *Upd* neurons (Figures 6B and S6). However, rhythmic regulation of the JAK/STAT pathway could be reinforced by clocks in other cells, e.g., those in which PER and *Upd*-GAL4 are coexpressed. In addition, *miR-279* may regulate more than just *Upd* in the JAK/STAT pathway (Yoon et al., 2011).

Our data now demonstrate a role of the JAK/STAT pathway in circadian rhythms. To date, most studies of signaling in the circadian system have focused on cAMP or mitogen-activated

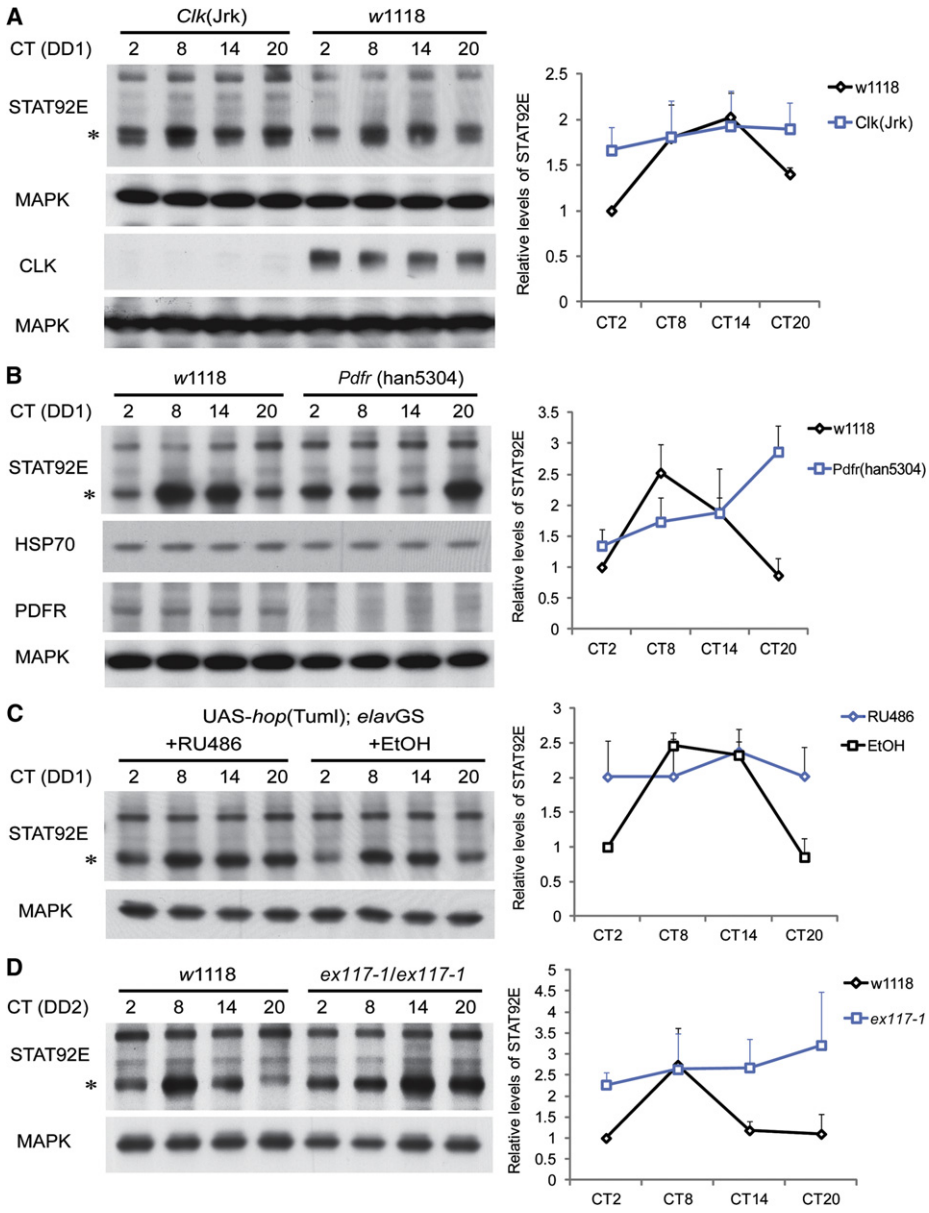

Figure 5. JAK/STAT Signaling Is downstream of the Central Clock and the PDFR

Flies of the indicated genotypes were collected at different circadian times (CT) on the 1st (DD1) or 2nd (DD2) day of DD. Protein extracts of brains were subjected to western blot analysis using antibodies specific for STAT92E and loading controls (MAPK or HSP70). Multiple bands are detected for STAT92E, of which the fastest mobility forms are expressed cyclically (indicated with asterisks). Each experiment was conducted three times, and quantified STAT92E and loading control levels were normalized to those at CT2 of wild-type controls in each gel. The quantification curves in each panel were plotted as the average ± standard error of the mean (SEM) of three independent western blots.

(A and B) STAT92E protein levels cycle in fly brains and are regulated by the circadian clock and PDFR. STAT92E levels at the trough (CT2 and CT20) are significantly lower than at the peak (CT8 and CT14) in w^{1118} control flies ($p < 0.01$), but not so in Clk^{Jrk} mutants ($p = 0.39$), as assessed by Student's t test (A). Although random fluctuations were observed in Clk^{Jrk} mutants, a 24 hr oscillation was not detected in any of multiple experiments. One-way ANOVA detects a significant cycle in both w^{1118} and $Pdfr^{han5304}$ mutants (B), and two-way ANOVA indicates that the oscillation is altered in $Pdfr^{han5304}$ ($p < 0.05$). The Clk^{Jrk} and $Pdfr^{han5304}$ mutations were confirmed by probing with CLK and PDFR antibodies using fly head extracts.

(C) The cycling of STAT92E is disrupted when hop^{TumI} is overexpressed in the adult nervous system. Five hundred micromoles of RU486 or ethanol (control) was administered in the food to induce *elav*GS from the time of entrainment. One-way ANOVA detects a cycle in the ethanol control ($p < 0.05$) but not in RU486-treated flies ($p = 0.93$).

(D) STAT92E protein levels continue to cycle on DD2 in wild-type flies, but the cycling is dampened in *miR-279* mutants. STAT92E levels at the peak (CT8) are significantly higher than at other time points (CT2, CT14, and CT20) in wild-type flies ($p < 0.01$), but not so in *ex117-1* flies ($p = 0.46$), as assessed by Student's t test. The daily expression of STAT92E in *ex117-1* flies is significantly different from that in w^{1118} flies ($p < 0.05$, by two-way ANOVA).

See also Figure S5.

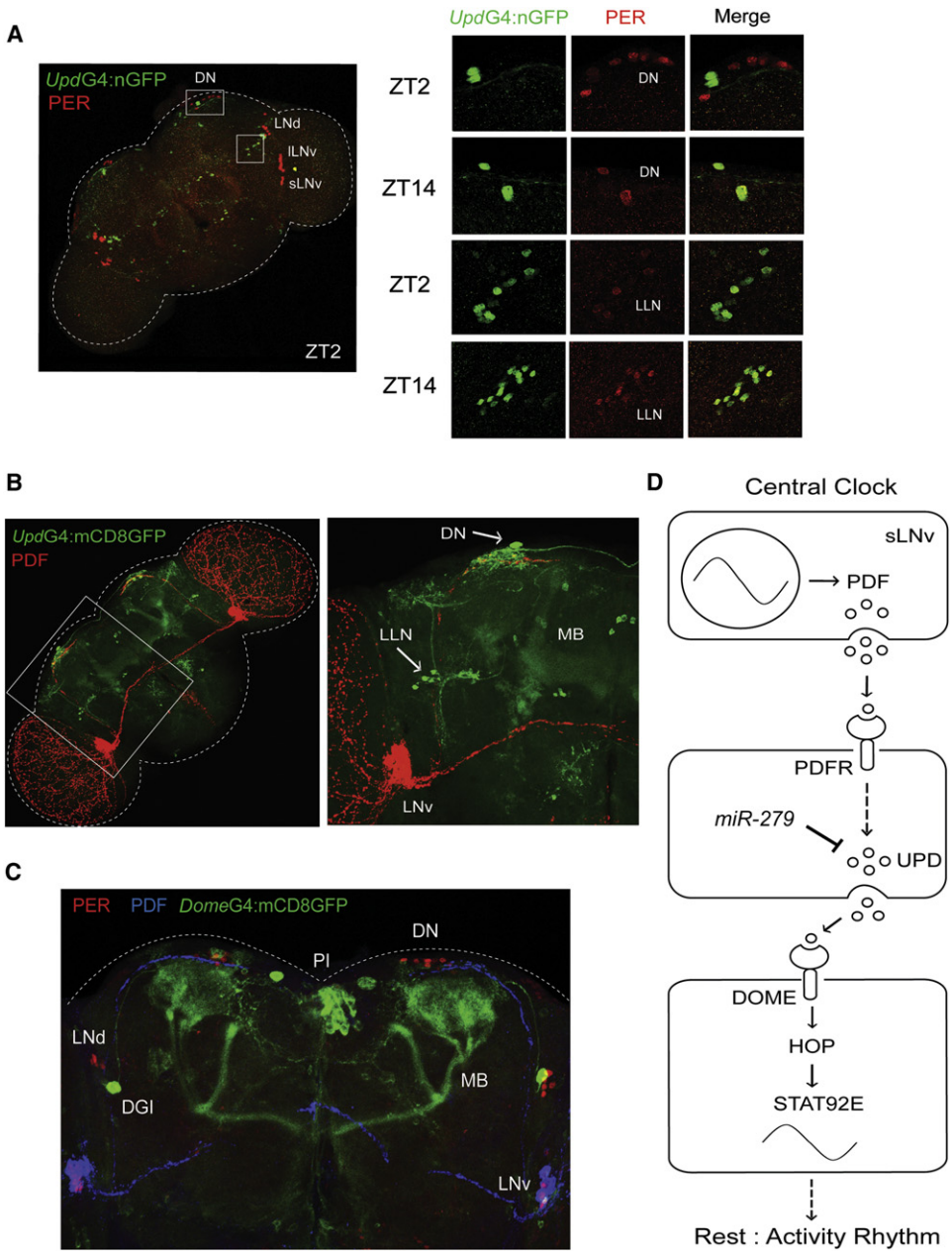

Figure 6. JAK/STAT Signaling and *miR-279* Are in a Circadian Output Circuit

(A) The expression pattern of *Upd* includes DNs and LLNs, which show shifted-phase expression of PER. Brains of *Upd*-GAL4:nGFP flies were dissected and stained with GFP (green) and PER (red) antibodies at indicated Zeitgeber times (ZT) on the 4th day in LD. PER protein levels are high in the early night in a subset of DNs and LLNs but high in the early morning in other clock neurons.

(B) PDF-containing dorsal projections from the central clock are in the vicinity of *Upd*-expressing neurons. A membrane-targeted mCD8GFP was expressed under the control of *Upd*-GAL4. Brains were dissected and stained with GFP (green) and PDF (red) antibodies. An enlarged image is shown on the right of the panel. *Upd*-expressing neurons are indicated with white arrows.

(C) *Dome* expresses in the MBs, PI, and DGIs. An mCD8GFP was expressed under the control of *Dome*-GAL4. Brains were dissected at ZT2 on the 4th day in LD and stained with GFP (green), PER (red), and PDF (blue) antibodies.

(D) Model depicting the role of *miR-279* and JAK/STAT signaling in a circadian behavioral output. We propose that the central clock affects cyclic secretion of the UPD protein from cells that act downstream of PDF signaling. The mRNA levels of *Upd* in these neurons are negatively modulated by *miR-279*. UPD may rhythmically activate the DOME receptor in *Dome*-expressing cells, which would lead to daily oscillations of JAK/STAT activity and therefore of STAT92E levels (see Discussion). Rhythmic activity of this pathway is likely required for rest:activity rhythm.

See also Figure S6.

protein kinase (MAPK) pathways, which may function in all aspects of circadian timekeeping (input to the clock, clock function, and output) (Allada and Chung, 2010). In the *Drosophila* circadian system, MAPK activity cycles in parts of the fly brain (Williams et al., 2001), and this appears to be related to the function of the Neurofibromatosis 1 (NF1) protein in circadian rhythms. Studies have shown that NF1 is required downstream of the clock for rhythmic rest:activity, and its effects on rhythms are mediated by the RAS/MAPK pathway (Williams et al., 2001). Interestingly, in mammalian glia and neural stem cells, NF1 influences STAT3 activity such that STAT3 signaling is hyperactivated in NF1-deficient cells (Banerjee et al., 2010). We do not know of a connection between NF1 and JAK/STAT in *Drosophila*, but as STAT92E fluctuates with a circadian rhythm in the fly brain, it is an intriguing possibility that the two are linked in the circadian system.

Upd and its receptor, *Dome*, are expressed widely in the fly brain. It is interesting, however, that *Upd* is coexpressed with PER in cells where PER cycles with a shifted phase under LD conditions. In these cells, PER cycles but is out of phase with other neurons, including those comprising the central clock. Two sites of *Upd* and PER coexpresssion are in some of the DNs and in neurons we have termed LLNs because of their lateral location. The function of these double-positive neurons is unclear at this time. The dorsal neurons are unlikely to be the DN2s because although PER expression in DN2s is antiphase in larvae, it cycles with a normal phase in adult flies (Kaneko et al., 1997). Likewise, the LLNs are probably not lateral posterior neurons (LPNs), located in the same region, because those are apparently three in number in each hemisphere and show normal PER cycling (Shafer et al., 2006). Based upon their position, the DNs that express *Upd* could represent a subset of the dorsal neuron cluster 1 (DN1s). Regardless of the precise cell types in which they are expressed, *Upd* and *Dome* expression provide tools to map the cellular circuitry of the output pathway that drives rhythmic rest:activity.

It is likely that many other microRNAs are involved in circadian rhythms. Because identification of such miRNAs will be difficult through traditional genetic screens, other approaches will have to be devised. Bioinformatics to identify miRNAs that target clock genes is obviously a viable method, but, as noted here, this approach typically identifies many possible targets for each miRNA, only some of which are biologically relevant. Thus, future computational analyses will need to be followed by many additional tests. Although this is doable, another caveat of this approach is that it will restrict analysis to miRNAs that target clock genes. Another approach is to identify miRNAs that are expressed cyclically. This was done recently in *Drosophila*, and it identified some miRNAs, which may turn out to be important regulators of circadian rhythms (Yang et al., 2008). In addition to these approaches, it will be important to completely dissect the circadian circuitry. Although we have an understanding of the components of the central clock and the mechanisms that entrain the clock to light, how clock signals are transduced to produce overt rhythms, in particular behavioral rhythms, is less well understood. Advances in this area, including those reported here, will provide a framework upon which whole circuits can be assembled.

EXPERIMENTAL PROCEDURES

Fly Strains and Behavioral Assays

Transgenic fly lines carrying either the *UAS-miR-279* (S) or *UAS-miR-279* (L) construct were generated by the site-specific PhiC31 Integration System (Rainbow Transgenics) using the attP landing site 2A on the X chromosome (Bischof et al., 2007). Fly lines obtained from other sources were outcrossed 5–7 times into an isogenic w^{1118} (iso31) strain. The EP insertion in NE95-11-24 was mapped by using inverse PCR and a cycle sequencing of P element insertions protocol (E. Jay Rehm, Berkeley *Drosophila* Genome Project). Locomotor activity rhythms were measured as previously described (Williams et al., 2001). Refer to the Extended Experimental Procedures for details.

Quantitative Real-time PCR

Fly heads or dissected fly brains were collected on dry ice and stored at −80°C until use. Total RNA, including miRNA, was purified with miRNeasy Mini kit (QIAGEN). Reverse transcription and real-time PCR of *miR-279* and 2s rRNA (or U27) were performed with TaqMan MicroRNA Assays designed for detecting mature miRNAs (Applied Biosystems). RT-PCR was performed on an ABI prism 7100 (Applied Biosystems). Refer to the Extended Experimental Procedures for details of other qPCR assays.

Whole-Mount Brain Immunocytochemistry

Adult fly brains were collected at indicated time points and fixed with 4% paraformaldehyde (PFA) in PBS. After three 15 min washes with 0.3% Triton X-100 in PBS, brains were blocked with 5% normal donkey serum. Samples were then incubated overnight at 4°C with primary antibodies. After three 20 min washes, brains were incubated with secondary donkey antibodies (Jackson ImmunoResearch Laboratories, 1: 1000) for 2 hr at room temperature, followed by extensive washes. Samples were imaged using a Leica TCS SP5 confocal microscope. Six to ten fly brains were examined for each time point. Representative images are shown. Refer to the Extended Experimental Procedures for details.

Western Blot Analysis

Ten to fourteen flies were exposed to microwave radiation for 2–3 min at indicated time points in DD. The eyes and fat bodies were carefully removed, and dissected fly brains were collected on dry ice. The brain samples were immediately subjected to protein extraction and western blots as previously described (Sathyanarayanan et al., 2004). The STAT92E and loading control bands were quantified using ImageJ software as previously described (Kojima et al., 2010). Western blot assays were repeated three times with similar results. Refer to the Extended Experimental Procedures for details.

Luciferase Reporter Assay in S2 Cells

The full-length 3′ UTR of *Upd* and a ~600 bp coding region of *miR-279* were amplified by PCR using AccuPrime Taq DNA Polymerase High Fidelity (Invitrogen). The *Upd* 3′ UTR was cloned into a pAc5.1-firefly luciferase-V5-His vector, and the *miR-279* coding region was cloned into a pAC5.1-V5-His vector (Invitrogen). The *miR-279* coding sequence was mutated using the Quickchange II XL Site-Directed Mutagenesis Kit (Agilent Technologies). Ten nanograms of pAc-firefly luc-*Upd* 3′ UTR, 90 ng pAc-*miR-279* (or empty vector control, or pAc-*miR-279* mutant), and 50 ng pAc-*Renilla* luc (transfection control) were cotransfected into S2 cells with Effectene Transfection Reagent (QIAGEN). Luciferase activity was measured using the Dual-Glo Luciferase Assay System (Promega). Refer to the Extended Experimental Procedures for details.

SUPPLEMENTAL INFORMATION

Supplemental Information includes Extended Experimental Procedures, six figures, and one table and can be found with this article online at doi:10.1016/j.cell.2011.12.024.

ACKNOWLEDGMENTS

We are very grateful to Zhaohai Yang and Zhifeng Yue for generating the NE95-11-24 fly line. We thank L. Zipursky, B. Edgar, D. Bilder, S. Hou, G. Baeg, T. Cline, W. Odenwald, I. Rebay, J. Blau, and M. Rosbash for providing *miR-279,* JAK/STAT, and other fly stocks; S. Hou, D. Harrison, P. Taghert, and P. Hardin for STAT92E, UPD, HOP, PDFR, and CLK antibodies; E. Izaurralde and K. Basler for pAc5.1-F. Luc and p*UAST*attB vectors; X. Zheng and D. Chen for developing PER antibodies; W. Joiner, A. Crocker, and S. Kumar for outcrossing some mutants and GAL4 lines; and other members of the laboratory for useful discussions. The work was supported by NIH grants 1-R560NS-048471 and 2R01NS04847. A.S. is an Investigator in the HHMI.

Received: April 19, 2011
Revised: October 28, 2011
Accepted: December 15, 2011
Published online: February 2, 2012

REFERENCES

Allada, R., and Chung, B.Y. (2010). Circadian organization of behavior and physiology in Drosophila. Annu. Rev. Physiol. *72*, 605–624.

Arbouzova, N.I., and Zeidler, M.P. (2006). JAK/STAT signalling in Drosophila: insights into conserved regulatory and cellular functions. Development *133*, 2605–2616.

Asher, G., and Schibler, U. (2011). Crosstalk between components of circadian and metabolic cycles in mammals. Cell Metab. *13*, 125–137.

Baines, R.A., Uhler, J.P., Thompson, A., Sweeney, S.T., and Bate, M. (2001). Altered electrical properties in Drosophila neurons developing without synaptic transmission. J. Neurosci. *21*, 1523–1531.

Banerjee, S., Byrd, J.N., Gianino, S.M., Harpstrite, S.E., Rodriguez, F.J., Tuskan, R.G., Reilly, K.M., Piwnica-Worms, D.R., and Gutmann, D.H. (2010). The neurofibromatosis type 1 tumor suppressor controls cell growth by regulating signal transducer and activator of transcription-3 activity in vitro and in vivo. Cancer Res. *70*, 1356–1366.

Bischof, J., Maeda, R.K., Hediger, M., Karch, F., and Basler, K. (2007). An optimized transgenesis system for Drosophila using germ-line-specific phiC31 integrases. Proc. Natl. Acad. Sci. USA *104*, 3312–3317.

Blau, J., and Young, M.W. (1999). Cycling *vrille* expression is required for a functional Drosophila clock. Cell *99*, 661–671.

Brown, S., Hu, N., and Hombría, J.C. (2001). Identification of the first invertebrate interleukin JAK/STAT receptor, the Drosophila gene domeless. Curr. Biol. *11*, 1700–1705.

Carthew, R.W., and Sontheimer, E.J. (2009). Origins and mechanisms of miRNAs and siRNAs. Cell *136*, 642–655.

Cayirlioglu, P., Kadow, I.G., Zhan, X., Okamura, K., Suh, G.S., Gunning, D., Lai, E.C., and Zipursky, S.L. (2008). Hybrid neurons in a microRNA mutant are putative evolutionary intermediates in insect CO2 sensory systems. Science *319*, 1256–1260.

Cheng, H.Y., Papp, J.W., Varlamova, O., Dziema, H., Russell, B., Curfman, J.P., Nakazawa, T., Shimizu, K., Okamura, H., Impey, S., and Obrietan, K. (2007). microRNA modulation of circadian-clock period and entrainment. Neuron *54*, 813–829.

Eskin, A. (1979). Identification and physiology of circadian pacemakers. Introduction. Fed. Proc. *38*, 2570–2572.

Ghiglione, C., Devergne, O., Georgenthum, E., Carballès, F., Médioni, C., Cerezo, D., and Noselli, S. (2002). The Drosophila cytokine receptor Domeless controls border cell migration and epithelial polarization during oogenesis. Development *129*, 5437–5447.

Halder, G., Callaerts, P., and Gehring, W.J. (1995). Induction of ectopic eyes by targeted expression of the eyeless gene in Drosophila. Science *267*, 1788–1792.

Hamada, F.N., Rosenzweig, M., Kang, K., Pulver, S.R., Ghezzi, A., Jegla, T.J., and Garrity, P.A. (2008). An internal thermal sensor controlling temperature preference in Drosophila. Nature *454*, 217–220.

Harmer, S.L. (2009). The circadian system in higher plants. Annu. Rev. Plant Biol. *60*, 357–377.

Harrison, D.A., Binari, R., Nahreini, T.S., Gilman, M., and Perrimon, N. (1995). Activation of a Drosophila Janus kinase (JAK) causes hematopoietic neoplasia and developmental defects. EMBO J. *14*, 2857–2865.

Harrison, D.A., McCoon, P.E., Binari, R., Gilman, M., and Perrimon, N. (1998). Drosophila unpaired encodes a secreted protein that activates the JAK signaling pathway. Genes Dev. *12*, 3252–3263.

Helfrich-Förster, C., Täuber, M., Park, J.H., Mühlig-Versen, M., Schneuwly, S., and Hofbauer, A. (2000). Ectopic expression of the neuropeptide pigment-dispersing factor alters behavioral rhythms in Drosophila melanogaster. J. Neurosci. *20*, 3339–3353.

Hou, X.S., Melnick, M.B., and Perrimon, N. (1996). Marelle acts downstream of the Drosophila HOP/JAK kinase and encodes a protein similar to the mammalian STATs. Cell *84*, 411–419.

Hyun, S., Lee, Y., Hong, S.T., Bang, S., Paik, D., Kang, J., Shin, J., Lee, J., Jeon, K., Hwang, S., et al. (2005). Drosophila GPCR Han is a receptor for the circadian clock neuropeptide PDF. Neuron *48*, 267–278.

Kadener, S., Menet, J.S., Sugino, K., Horwich, M.D., Weissbein, U., Nawathean, P., Vagin, V.V., Zamore, P.D., Nelson, S.B., and Rosbash, M. (2009). A role for microRNAs in the Drosophila circadian clock. Genes Dev. *23*, 2179–2191.

Kaneko, M., Helfrich-Förster, C., and Hall, J.C. (1997). Spatial and temporal expression of the period and timeless genes in the developing nervous system of Drosophila: newly identified pacemaker candidates and novel features of clock gene product cycling. J. Neurosci. *17*, 6745–6760.

Koenig, J.H., Saito, K., and Ikeda, K. (1983). Reversible control of synaptic transmission in a single gene mutant of Drosophila melanogaster. J. Cell Biol. *96*, 1517–1522.

Kojima, S., Gatfield, D., Esau, C.C., and Green, C.B. (2010). MicroRNA-122 modulates the rhythmic expression profile of the circadian deadenylase Nocturnin in mouse liver. PLoS ONE *5*, e11264.

Krek, A., Grün, D., Poy, M.N., Wolf, R., Rosenberg, L., Epstein, E.J., MacMenamin, P., da Piedade, I., Gunsalus, K.C., Stoffel, M., and Rajewsky, N. (2005). Combinatorial microRNA target predictions. Nat. Genet. *37*, 495–500.

Luo, H., Hanratty, W.P., and Dearolf, C.R. (1995). An amino acid substitution in the Drosophila hopTum-l Jak kinase causes leukemia-like hematopoietic defects. EMBO J. *14*, 1412–1420.

Luo, H., Asha, H., Kockel, L., Parke, T., Mlodzik, M., and Dearolf, C.R. (1999). The Drosophila Jak kinase hopscotch is required for multiple developmental processes in the eye. Dev. Biol. *213*, 432–441.

McGuire, S.E., Mao, Z., and Davis, R.L. (2004). Spatiotemporal gene expression targeting with the TARGET and gene-switch systems in Drosophila. Sci. STKE *2004*, pl6.

Nicolaï, L.J., Ramaekers, A., Raemaekers, T., Drozdzecki, A., Mauss, A.S., Yan, J., Landgraf, M., Annaert, W., and Hassan, B.A. (2010). Genetically encoded dendritic marker sheds light on neuronal connectivity in Drosophila. Proc. Natl. Acad. Sci. USA *107*, 20553–20558.

Nitabach, M.N., and Taghert, P.H. (2008). Organization of the Drosophila circadian control circuit. Curr. Biol. *18*, R84–R93.

Park, J.H., Helfrich-Förster, C., Lee, G., Liu, L., Rosbash, M., and Hall, J.C. (2000). Differential regulation of circadian pacemaker output by separate clock genes in Drosophila. Proc. Natl. Acad. Sci. USA *97*, 3608–3613.

Perrimon, N., and Mahowald, A.P. (1986). l(1)hopscotch, A larval-pupal zygotic lethal with a specific maternal effect on segmentation in Drosophila. Dev. Biol. *118*, 28–41.

Ren, D., Navarro, B., Xu, H., Yue, L., Shi, Q., and Clapham, D.E. (2001). A prokaryotic voltage-gated sodium channel. Science *294*, 2372–2375.

Ruby, J.G., Stark, A., Johnston, W.K., Kellis, M., Bartel, D.P., and Lai, E.C. (2007). Evolution, biogenesis, expression, and target predictions of a substantially expanded set of Drosophila microRNAs. Genome Res. *17*, 1850–1864.

Sathyanarayanan, S., Zheng, X., Xiao, R., and Sehgal, A. (2004). Posttranslational regulation of Drosophila PERIOD protein by protein phosphatase 2A. Cell *116*, 603–615.

Shafer, O.T., Helfrich-Förster, C., Renn, S.C., and Taghert, P.H. (2006). Reevaluation of Drosophila melanogaster's neuronal circadian pacemakers reveals new neuronal classes. J. Comp. Neurol. *498*, 180–193.

Shi, L., Ko, M.L., and Ko, G.Y. (2009). Rhythmic expression of microRNA-26a regulates the L-type voltage-gated calcium channel alpha1C subunit in chicken cone photoreceptors. J. Biol. Chem. *284*, 25791–25803.

Vitalini, M.W., de Paula, R.M., Park, W.D., and Bell-Pedersen, D. (2006). The rhythms of life: circadian output pathways in Neurospora. J. Biol. Rhythms *21*, 432–444.

Williams, J.A., Su, H.S., Bernards, A., Field, J., and Sehgal, A. (2001). A circadian output in Drosophila mediated by neurofibromatosis-1 and Ras/MAPK. Science *293*, 2251–2256.

Yang, M., Lee, J.E., Padgett, R.W., and Edery, I. (2008). Circadian regulation of a limited set of conserved microRNAs in Drosophila. BMC Genomics *9*, 83.

Yang, Z., and Sehgal, A. (2001). Role of molecular oscillations in generating behavioral rhythms in Drosophila. Neuron *29*, 453–467.

Yoon, W.H., Meinhardt, H., and Montell, D.J. (2011). miRNA-mediated feedback inhibition of JAK/STAT morphogen signalling establishes a cell fate threshold. Nat. Cell Biol. *13*, 1062–1069.

Zheng, X., and Sehgal, A. (2008). Probing the relative importance of molecular oscillations in the circadian clock. Genetics *178*, 1147–1155.

Zheng, X., Yang, Z., Yue, Z., Alvarez, J.D., and Sehgal, A. (2007). FOXO and insulin signaling regulate sensitivity of the circadian clock to oxidative stress. Proc. Natl. Acad. Sci. USA *104*, 15899–15904.